Genetic Algorithm Applied to State-Feedback Control Design of Grid and Circulating Current in Modular Multilevel Converters

Ghassani, Rashad; Bratcu, Antoneta Iuliana; Teodorescu, Remus

Published in:
IFAC-PapersOnLine

DOI (link to publication from Publisher):
10.1016/j.ifacol.2022.07.075

Publication date:
2022

Document Version
Publisher's PDF, also known as Version of record

Available online at www.sciencedirect.com

ScienceDirect

IFAC PapersOnLine 55-9 (2022) 431–436

Genetic Algorithm Applied to State-Feedback Control Design of Grid and Circulating Current in Modular Multilevel Converters

Rashad Ghassani * Antoneta Iuliana Bratcu *
Remus Teodorescu **

* *Univ. Grenoble Alpes (UGA), CNRS, Grenoble INP, GIPSA-lab, 38402, Saint-Martin d'Hères Cedex, France*
Institute of Engineering Univ. Grenoble Alpes, (e-mail: rashad.ghassani@gipsa-lab.grenoble-inp.fr), (Tel: +33476826384; e-mail: antoneta.bratcu@gipsa-lab.grenoble-inp.fr)
** *Department of Energy Technology, Aalborg University, Aalborg, Denmark, (e-mail: ret@et.aau.dk)*

Abstract: This paper discusses the application of a genetic algorithm (GA) to control system design for Modular Multilevel Converters (MMCs). In particular, genetic algorithm is used to compute the gains of a state-feedback controller for multi-input/multi-output (MIMO) plant model. This GA-optimized state-feedback controller is used to control both grid and circulating current of the MMC. This assures that the two currents' input-coupled dynamics are managed using a MIMO strategy. A detailed MATLAB®/Simulink® model of a three-phase MMC is further used to validate the proposed control technique. Different simulations show that the GA-optimized state-feedback controller outperforms the conventional cascaded control.

Keywords: modular multilevel converter, cascaded control, state-feedback, genetic algorithm

1. INTRODUCTION

With the fast improvement of wind farms, the request for high-power, high-quality transmission systems is becoming more urgent. Modular Multilevel Converter (MMC) which is based on high-voltage direct-current (HVDC) innovation gives a promising solution (Lesnicar and Marquardt (2003)). In recent years, MMCs have become one of the most appealing topologies for high-voltage industrial applications such as HVDC, medium-voltage motor drives, and energy storage systems. The modularity, flexible expandability, transformer-less architecture, and low cost of MMCs have all contributed to their widespread acceptance in the industry.

Controlling the transferred power through the MMC to the grid is the main objective. Two control structures have been proposed in the literature, which are multi-variable (Munch et al. (2010)) and cascaded (Bergna Diaz et al. (2013)) approaches. The first approach allows to handle the MMC state-space equations as a nonlinear multi-variable model. It requires some advanced control strategies in order to derive the associated control law and perform stability analysis. The second approach, which is based on different time scales assumptions, treats the system in a decoupled way, such that the control algorithm is created and modified step by step (Yijing et al. (2014)).

The cascaded approach in dealing with all the different variables of MMC MIMO plant is the most preferred approach in the industry. The control design approach to MIMO systems requires the state space representation, in which the state feedback control is used. The most commonly used strategy for state-feedback control design is the Linear Quadratic Regulation (LQR) (Solihin et al. (2010)). Despite the positive results produced by this approach, control design is a difficult process due to the trial-and-error method used in the weight matrix creation where hard tuning the controller parameters could be tedious task. However, using Artificial Intelligent (AI) control design techniques can be a promising alternative. Control-design approaches make use of this domain knowledge for the control application to come up with a control system that minimizes some weighted performance function. The genetic algorithm (GA) is heuristic search method that holds a great potential in the control system design problem (Sivanandam and Deepa (2007)).

This paper proposes a new optimal control strategy for a MIMO state-feedback controller that controls both grid and circulating current using GA to find the controller gains. The state-feedback optimization problem is solved under the balanced-grid model, but it is tested under the unbalanced conditions. This paper is organized as follows. Section 2 introduces the balanced-grid three-phase MMC model, which is used later to design the proposed GA-optimized MIMO state-feedback controller in Section 3. Section 4 discusses the GA setup and calibration. Section 5 shows the results obtained on a comprehensive MATLAB®/Simulink® three-phase MMC model. The conclusion is presented in the last Section 6.

10.1016/j.ifacol.2022.07.075

2. MMC CURRENT STATE EQUATIONS

A detailed diagram of a typical three-phase MMC is shown in Figure 1. Each arm consists of N sub-modules (SM), the arm resistance (adding the losses within each arm) and arm inductance. The voltage of each SM, that is composed of a two semiconductors switches and a capacitor, is defined by $v_{k,j}$, where subscript k represents the converters arms ($k = u, l$, upper arm and lower arm respectively) and subscript j represents phase ($j = a, b, c$). On the ac side, the converter is assumed to be connected to the grid. The dc side of converter is grounded at its midpoint. Using Kirchhoff voltage law (KVL), the dynamic equations of MMC system in each phase can be expressed by:

$$\frac{v_d}{2} - v_u - Ri_u - L\frac{di_u}{dt} = v_a \qquad \frac{-v_d}{2} + v_l + Ri_l + L\frac{di_l}{dt} = v_a \tag{1}$$

In Figure 1, each sub-module capacitor is represented by an (A-B) Block. Different MMC parameters can be summarized as follows: dc variables (current and voltage) are represented by the subscript "d", ac variables for each phase are denoted by $v_{a,b,c}$. The number of sub-modules in each arm is N, while the resistance and inductance of the arm are R and L, respectively.

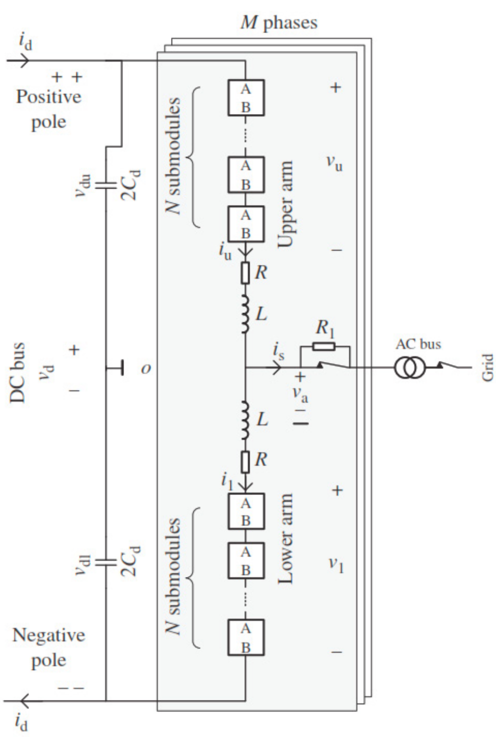

Fig. 1. Structure of a typical three-phase MMC, showing all the important variables including the dc and ac bus Sharifabadi et al. (2016)

For each phase, the voltage for a single SM_i is denoted as $v^i_{cu,l}$ for the upper and lower arm with an insertion index defined as $n^i_{u,l} = 1$ if the SM is inserted and 0 otherwise. The total arm voltage can be defined as total number of inserted capacitor SMs such that $v_{u,l} = \sum_{i=1}^{N} n^i_{u,l} \cdot v^i_{cu,l}$ and the sum of capacitor voltages on an arm is defined as $v^{\Sigma}_{cu,l} = \sum_{i=1}^{N} v^i_{cu,l}$, while the insertion index in an arm is defined as $n_{u,l} = (1/N)\sum_{i=1}^{N} n^i_{u,l}$. Assuming that all capacitor voltages are equal, and combining the above-mentioned formulas, the following conclusion holds: $v_{u,l} = n_{u,l} \cdot v^{\Sigma}_{cu,l}$. Therefore, the output current i_s and output voltage v_s can be written as:

$$i_s = i_u - i_l, v_s = (v_u - v_l)/2 \tag{2}$$

and the circulating current i_c and internal voltage v_c can be defined as:

$$i_c = (i_u + i_l)/2, v_c = (v_u + v_l)/2 \tag{3}$$

Based again on Figure 1 and Equations (1), (2), and (3), the dynamic equations of MMC for phase j can be expressed by:

$$\begin{cases} \dot{i_c} = -R/L \cdot i_c - 1/(2L) \cdot v_u - 1/(2L) \cdot v_l + 1/(2L) \cdot v_d \\ \dot{i_s} = R/L \cdot i_s - 1/L \cdot v_u - 1/L \cdot v_l - 2/L \cdot v_a \end{cases} \tag{4}$$

Replacing v_s from (2) and v_c from (3), (4) is obtained. It can be shown that the circulating current i_c follows a first-order dc-dynamics and output current i_s obeys a first-order ac-circuit dynamics.

$$\dot{i_c} = -R/L \cdot i_c - v_c/L + 1/(2L) \cdot v_d \tag{5}$$
$$\dot{i_s} = -R/L \cdot i_s + 2/L \cdot v_s - 2/L \cdot v_a \tag{6}$$

The two currents can be regulated individually using proportional integral (PI) or proportional-resonant (PR) linear controllers by employing v_c in (2) and v_s in (3) as control inputs Sharifabadi et al. (2016).

3. STATE-FEEDBACK CONTROL DESIGN

In this section, the state-feedback controller (Bratcu and Teodorescu (2020)), is introduced. Starting from the state equations (5) and (6) characterizing the dynamics of the two currents on a single phase, a new control design can be made. It is worth noting that these dynamics are intertwined at the input level: upper and lower-arm voltages intervene in both, which will now be the control inputs. On the second-order system, dc voltage v_d acts as a constant disturbance, whereas voltage v_a is perceived as a grid-frequency sinusoidal disturbance.

$$\begin{cases} \dot{i_c} = -R/L \cdot i_c - 1/(2L) \cdot v_u - 1/(2L) \cdot v_l + 1/(2L) \cdot v_d \\ \dot{i_s} = R/L \cdot i_s - 1/L \cdot v_u - 1/L \cdot v_l - 2/L \cdot v_a \end{cases} \tag{7}$$

For the MIMO plant (7), a full-state feedback is developed to achieve the necessary closed-loop dynamics (Bratcu and Teodorescu (2020)). In order to place the desired closed-loop dynamics and to achieve the required control objectives: ensuring a constant-reference tracking for the dc-component of i_c, a ω-sinusoidal-reference tracking for i_s, as well as a 2ω-sinusoidal disturbance rejection on i_c. To this end, five extra integral states were added to achieve the desired objectives as follows:

$$\begin{cases} \dot{x}_{i1} = -x_{i2} + i_s^* - i_s \\ \dot{x}_{i2} = \omega^2 \cdot x_{i1} \\ \dot{x}_{i3} = i_c^* - i_c \\ \dot{x}_{i4} = -x_{i5} + i_c^* - i_c \\ \dot{x}_{i5} = 4\omega^2 \cdot x_{i4} \end{cases} \tag{8}$$

States x_{i1} and x_{i2} correspond to a resonant integrator on the grid frequency ω, state x_{i3} is that of an ordinary integrator that tries to eliminate the dc steady state error and finally, states x_{i4} and x_{i5} refer to a resonant integrator on double the grid frequency, 2ω. This combination between state-feedback control and resonant integrators can be seen as alternative to the classical integrators.

The MMC model can be represented by MIMO extended plant with $\mathbf{x_e} = [i_c \quad i_s \quad x_{i1} \quad x_{i2} \quad x_{i3} \quad x_{i4} \quad x_{i5}]^T$ as state variables, $\mathbf{u_e} = [v_u \quad v_l]^T$ as control input vector and $\mathbf{u_p} = [v_d \quad v_a]^T$ as disturbance input vector. Thus, the whole MIMO system can be described as $\dot{\mathbf{x}}_\mathbf{e} = \mathbf{A_e} \cdot \mathbf{x_e} + \mathbf{B_e} \cdot \mathbf{u_e} + \mathbf{B_p} \cdot \mathbf{u_p}$, where the state matrix $\mathbf{A_e}$ and input matrices $\mathbf{B_e}$ and $\mathbf{B_p}$ are as follows:

$$A_e = \begin{bmatrix} -R/L & 0 & 0 & 0 & 0 & 0 & 0 \\ 0 & -R/L & 0 & 0 & 0 & 0 & 0 \\ 0 & -1 & 0 & -1 & 0 & 0 & 0 \\ 0 & 0 & \omega^2 & 0 & 0 & 0 & 0 \\ -1 & 0 & 0 & 0 & 0 & 0 & 0 \\ -1 & 0 & 0 & 0 & 0 & 0 & -1 \\ 0 & 0 & 0 & 0 & 0 & 4\omega^2 & 0 \end{bmatrix}$$

$$B_e = \begin{bmatrix} -1/(2L) & -1/L & 0 & 0 & 0 & 0 & 0 \\ -1/(2L) & -1/L & 0 & 0 & 0 & 0 & 0 \end{bmatrix}^T$$

$$B_p = \begin{bmatrix} 1/(2L) & 0 & 0 & 0 & 0 & 0 & 0 \\ 0 & -2/L & 0 & 0 & 0 & 0 & 0 \end{bmatrix}^T$$

After ensuring that the extended system (A_e, B_e) is controllable, a full state-feedback controller of the form $\mathbf{u_e} = -\mathbf{K_e} \cdot \mathbf{x_e}$ can be computed to impose the desired closed-loop dynamics Bratcu and Teodorescu (2020). Two of the new poles correspond to the original second-order dynamics of both currents, i_c and i_s, the other five poles correspond to the integral states. Vector control input is $\mathbf{u_e} = [v_u^* \quad v_l^*]^T$. Internal voltage $v_c^* = (v_u^* + v_l^*)/2$ and grid voltage $v_s^* = (v_l^* - v_u^*)/2$ are computed, then sent as references to the modulation process, in order to obtain the desired upper and lower arm indices n_u^* and n_l^*, respectively.

The biggest challenge in this proposed state-feedback controller is how to choose the imposed closed-loop poles, because this choice will determine the control gain vector, $\mathbf{K_e}$. In the next section, a genetic algorithm technique is proposed to find the controller gains, which are optimal in view of a suitably defined criterion.

4. PROPOSED GENETIC-ALGORITHM-BASED COMPUTATION OF GAINS

Genetic Algorithms (GA) are based on Darwin's ideas of natural selection and evolutionary processes. Only the fittest individuals survive in a selection process, leaving the poor performers behind. The cost function is commonly referred to as a *fitness* function, and the process of *'survival of the fittest'* entails a maximization approach. A GA begins by random population of initial solutions, and then applies a series of operations to generate a new population. Following that, the worst individuals are eliminated from the population, while the best ones are included in the next generation (Sivanandam and Deepa (2007)).

4.1 Fitness Function

As stated earlier, the GA begins with a purely random initial population; in this case the initial population is a pool of the closed-loop poles to be optimized. Using some cost function each candidate solution (set of poles) is evaluated in the initial population, the top elite candidates are then transferred directly to the new generation, while the other individuals undergo different genetic algorithm operators such as *crossover*, in which two individuals from the initial population (parents) are reproduced to produce two new individuals (children), and *mutation* which yields a new intermediate generation. The next generation is formed by applying these same rules, and the process is repeated until a convergence criterion is reached. Using GA-based techniques, a way to find the state-feedback controller gains to meet the design specifications is proposed in this work. The suggested approach is used to determine the appropriate state-feedback parameters and eliminate the time-consuming and repetitive trial-and-error procedure. As a result, no weight matrices must be chosen as in the LQR technique. The output current and circulating current tracking error are the chosen design specifications. So, it is proposed that the *fitness* function to take into account the circulating current and output current error as follows:

$$J = \frac{1}{N_s} \sum_{i=1}^{N_s} k_1 \cdot |i_{c_i} - i_c^*| + \frac{1}{N_s} \sum_{i=1}^{N_s} k_2 \cdot |i_{s_i} - i_s^*| \qquad (9)$$

where k_1 and k_2 are weights to be adjusted, i_c^* and i_s^* are the circulating current and output current references respectively, while N_s is the number of samples in the finite-horizon model.

As previously stated, the proposed MIMO extended MMC plant contains 7 states and 2 control inputs, the "optimal" feedback matrix $\mathbf{K_e}$ to be found is represented by 14 variables. The optimal closed-loop poles are found first using the proposed GA and after that the state-feedback control gain $\mathbf{K_e}$ is calculated. Algorithm 1 presents the different steps of the optimization procedure. The crossover probability P_c, mentioned in line 6, is equal to 0.9, while the mutation probability P_m is chosen to be equal to 0.3. The chosen population size is 120 and the number of generations is set to 50. Since it is equally important to control both currents, the weight parameters k_1 and k_2 are fixed to 1. The different steps of the proposed GA can be summarized as follows: first of all, the initial purely random and bounded population P_0 is created. After that, the evaluation of all the candidate poles is started. This evaluation process is done by running off-line the complete MMC simulation model presented in Appendix A for a time of 1 s under normal grid conditions, by using the candidate poles to be evaluated. As it is run off-line, this algorithm can work for any number of submodules per arm, N. This process is then repeated for all the population.

5. RESULTS AND NUMERICAL SIMULATIONS

The genetic algorithm optimization effectively identified the MIMO optimum controller's feedback gains after passing through 50 generations and calculating for around two

Algorithm 1: Proposed genetic algorithm

Input: **P**-population of individuals: pool of random poles bounded with upper and lower bound
Output: Best individual ("optimal" closed-loop poles in term of fitness function)
Initialize $t = 0$;
Create an initial population P_0;
Evaluate individuals - Calculate the value of fitness function for each individual in the population P_0;
while $t < Number\ of\ iterations\ and\ Stop\ Condition$ ***Not*** *Reached* **do**
  Select 5 elite individuals for new population;
  Crossover operation with a probability P_c;
  Mutation of individuals with a probability P_m;
  foreach $\mathbf{x} \in \mathbf{P_t}$ **do**
    Run the MMC model simulation for 1 s;
    Compute $fitnessFunction\ J$
  Replace the old population with new one;
  $t = t + 1$;

hours. The 7-variable vector of the imposed closed-loop poles results from the proposed genetic algorithm. The feedback matrix $\mathbf{K_e}$ is then easily computed using pole placement, while $\mathbf{K_{e\_3phase}}$, the three-phase extension of single phase gain $\mathbf{K_e}$, is used as the feedback gain matrix to the optimized state-feedback controller.

A detailed MATLAB®/Simulink® model of a three-phase MMC, whose parameters are presented in Appendix A, is used to validate the suggested control technique. The traditional control system, which is commonly used in practice and is based on many cascaded control levels Sharifabadi et al. (2016), is used as a baseline here. Indeed, the suggested state-feedback controller substitutes the two distinct control loops of i_c and i_s, while preserving other control levels present in the global multiple-level-based control method. As a result, the energy control level, as well as PWM modulation implementation, are preserved. The chosen scenario to test the proposed approach is set at 1.3 s, with an imbalance in grid conditions starting at time 0.7 s and ending at time 1.1 s. The balanced grid is defined by grid voltage positive sequence $v_{g\_pos} = 1$ p.u. and a voltage negative sequence $v_{g\_neg} = 0$ p.u., while the unbalance grid is characterized by a positive sequence $v_{g\_pos} = 0.8$ p.u. and a negative sequence $v_{g\_neg} = 0.2$ p.u..

5.1 GA-optimized state-feedback control results

The MIMO full-state feedback based on genetic algorithm is compared with the conventional cascaded control under the same relevant scenarios. The variables of interest are the output current i_s (both positive and negative sequence) and the internal dynamics, which contains the circulating current i_c, energy sum of each phase W_Σ, energy difference W_Δ, and sum capacitor voltage.

Figure 2 shows internal control results when traditional control is used. It is obvious that, once the voltage is unbalanced (0.7 s), the control is no longer functional. As a result, oscillations in the three-phase circulating current (second plot) and the sum of capacitors voltages (first plot) are increasing in amplitude and this leads to instability. Control of the energy sum W_Σ (third plot) is slow and has some steady-state error. Meanwhile, the control of energy difference has a lot of variance from zero reference. Results of internal control through the proposed method are shown in Figure 3 (same variables as before). It is noticed that, after the fault occurs, the closed-loop behavior is stabilized. Two of the circulating currents stabilize at about the same value, while that of the third phase stabilizes at a larger steady-state value.

Figure 4 shows the grid negative-sequence current i_s^- when conventional control is used. The result shows the closed-loop performance of the grid current negative sequence d and q axis components, while in the case of GA-optimized state-feedback control it is obvious that in Figure 5 the proposed controller improves the negative sequence grid reference tracking in terms of accuracy and transients between faulty and normal grid circumstance, which has a good influence on power evolution. Note that, only the negative sequence current is shown, while both controllers have similar effects on the positive sequence.

In Figures 6 and 7 the results for the circulating current i_c and energy difference W_Δ for phase c are introduced (similar results in the other two phases). This result indicates that the proposed GA performance is comparable to that of the standard conventional control, and even better when the fault occurs, the cascaded control tending to be unstable in such condition.

5.2 Simulation-Based Robustness Checking

To perform the simulation-based robustness checking, a parameter study is performed, that is, it is supposed that some parameters may vary in some ranges. The uncertainty system parameters has also been investigated for the same test scenario. For instance, the sub-module capacitance C, the arm's inductance L, and the arm's resistance R were let to vary randomly within +/- 20%, around their nominal values. The performance of the proposed GA optimized state-feedback controller being tested under these conditions Figure 8 for the circulating current i_c. As can be seen, the controller's dynamics response is still pretty good. The controller obtained with a parameter inaccuracy converges to the desired reference but with some higher ripples. This result suggests that the circulating current using the proposed controller converges to a boundary layer near the specified reference. A systematic robustness study should confirm this result.

6. CONCLUSION

In this paper, a GA-optimized MIMO state-feedback control of both the grid and the circulating current in MMCs has been proposed. This approach can be seen as an alternative to the LQR and pole placement methods. Although the proposed approach requires some computation time to identify the "optimal" poles, this will be done just once and in an off-line way. Furthermore, there are very few parameters to tune which can save a lot of design time. Under imbalanced grid configurations, simulations reveal improved performance as compared to the traditional control. Future work should focus on developing a control method that takes explicitly account of positive, negative, and zero sequences.

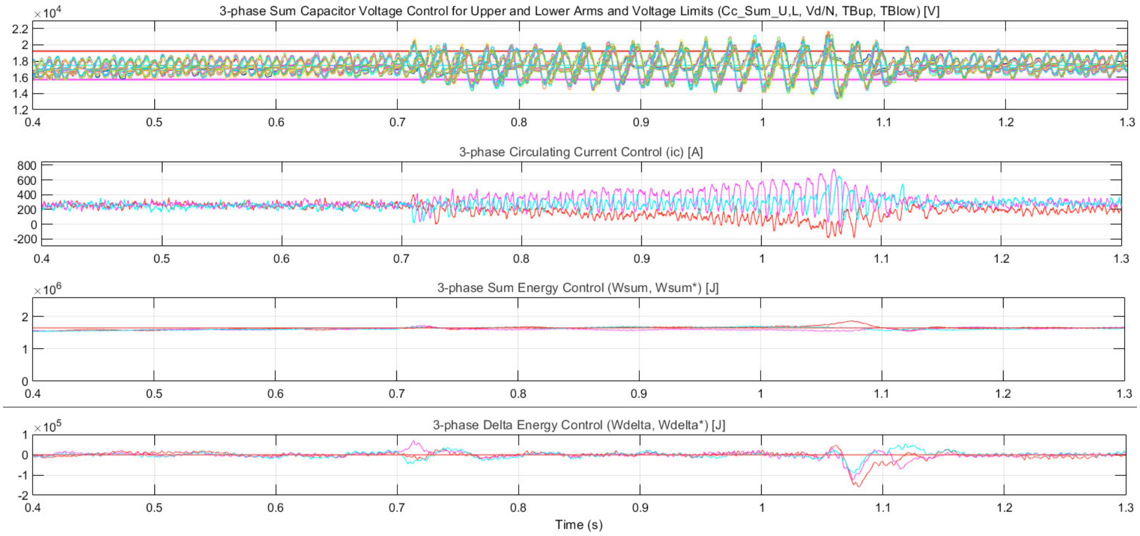

Fig. 2. Simulation results obtained for the *cascaded conventional internal control* of both i_c and i_s, under unbalanced grid conditions starting at time 0.7 s and lasting for 0.4 s

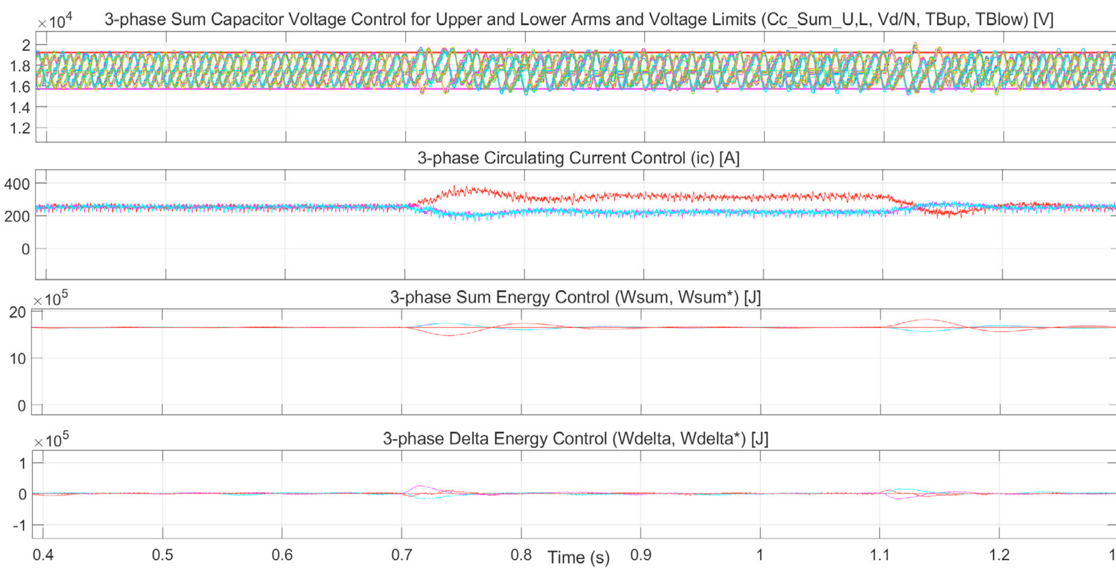

Fig. 3. Simulation results obtained for the *MIMO GA-optimized state-feedback internal control* of both i_c and i_s, under unbalanced grid conditions starting at time 0.7 s and lasting for 0.4 s

REFERENCES

Bergna Diaz, G., Berne, E., Egrot, P., Lefranc, P., Arzande, A., Vannier, J., and Molinas, M. (2013). An energy-based controller for hvdc modular multilevel converter in decoupled double synchronous reference frame for voltage oscillation reduction. *IEEE Transactions on Industrial Electronics*, 60, 2360–2371.

Bratcu, A.I. and Teodorescu, R. (2020). State-feedback control of grid and circulating current in modular multilevel converters. In *IFAC-PapersOnLine*, volume **53**, Issue 2, 2020, pp 12396-12401. Berlin, Germany.

Lesnicar, A. and Marquardt, R. (2003). An innovative modular multilevel converter topology suitable for a wide power range. *2003 IEEE Bologna Power Tech Conference Proceedings,*, 3, pp. 1–6.

Munch, P., Gőrges, D., Izak, M., and Liu, S. (2010). Integrated current control, energy control and energy balancing of modular multilevel converters. *IECON 2010 - 36th Annual Conference on IEEE Industrial Electronics Society*, 150–155.

Sharifabadi, K., L., H., Nee, H.P., Norrga, S., and Teodorescu, R. (2016). *Design, Control and Application of Modular Multilevel Converters for HVDC Transmission Systems*.

Sivanandam, S.N. and Deepa, S.N. (2007). *Introduction to Genetic Algorithms*. Springer Publishing Company, Incorporated, 1st edition.

Solihin, M.I., Wahyudi, Legowo, A., and Akmeliawati, R. (2010). Comparison of lqr and pso-based state feedback controller for tracking control of a flexible link manipulator. In *2010 2nd IEEE International Conference on Information Management and Engineering*, 354–358.

Yijing, C., Damm, G., Benchaib, A., Netto, M., and Lamnabhi-Lagarrigue, F. (2014). Control induced explicit time-scale separation to attain dc voltage stability for a vsc-hvdc terminal. *IFAC Proceedings*, 47, 540–545.

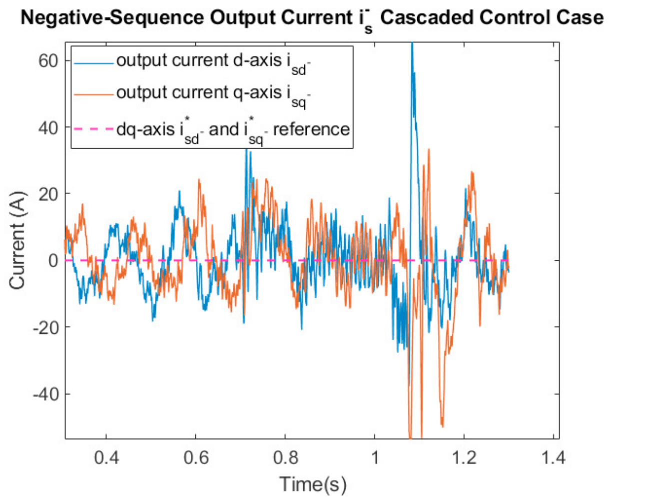

Fig. 4. Negative-sequence output current i_s^- $(d-q$ axis) control the case of conventional control

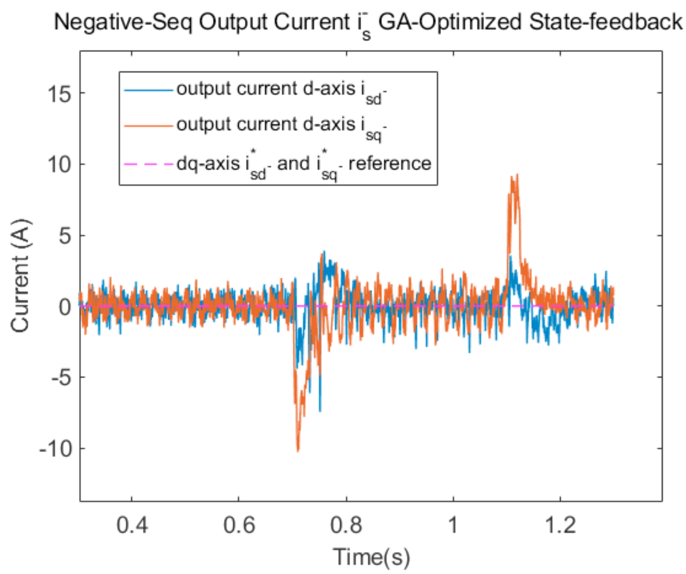

Fig. 5. Negative-sequence output current i_s^- $(d-q$ axis) control in the case of GA-optimized feedback control

Appendix A. THREE-PHASE MMC MODEL PARAMETERS

Electrical parameters

Rated apparent power S_{rated}=150 MVA; DC-bus voltage v_d=200 kV; grid frequency ω=$2\pi\cdot50$ rad/s; number of SMs N=12; arm resistance R=3.2 Ω; arm inductance L=50.9 mH; grid inductance L_g=3.2 mH; SM capacitance C=450 µF; Open-loop poles: –31.415, –31.415 (rad/s)

Control parameters

Open-loop poles: –31.415, –31.415 (rad/s)
Imposed closed-loop poles: –1322.68, –2240.46, –84.37, –691.24, –1059.26, –187.22, –2824.61 (rad/s)

Genetic Algorithm parameters

Dimension vector: 7, number of population: 120, number of generations: 50, probability of crossover P_c = 0.9, probability of mutation P_m = 0.3, upper bound= –5000 rad/s, lower bound –31.4159 rad/s (open-loop poles).

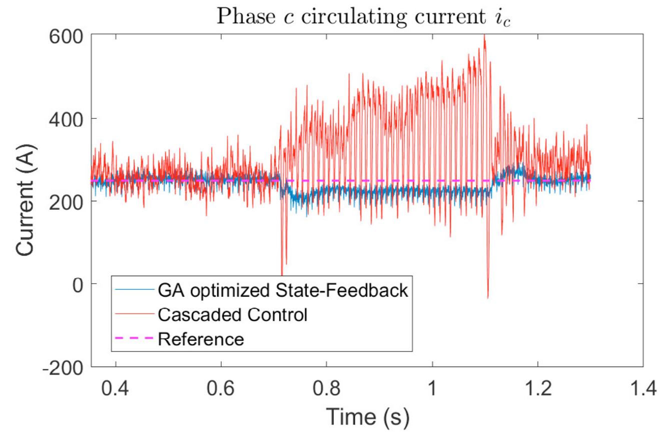

Fig. 6. Phase c circulating current i_c control: comparison between conventional and GA-optimized state-feedback control under unbalanced grid conditions

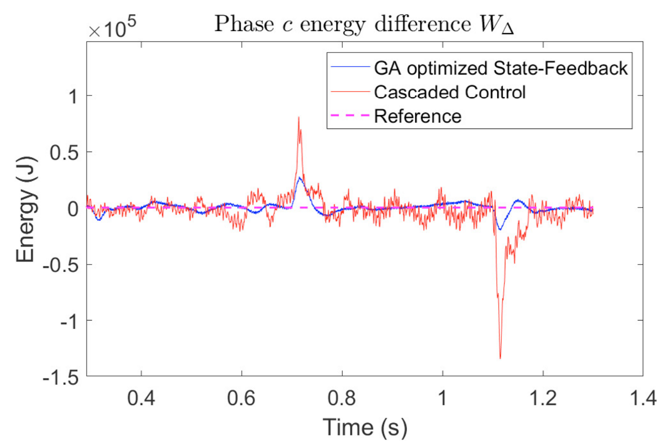

Fig. 7. Phase c energy difference W_Δ control: comparison between conventional and GA-optimized state-feedback control under unbalanced grid conditions

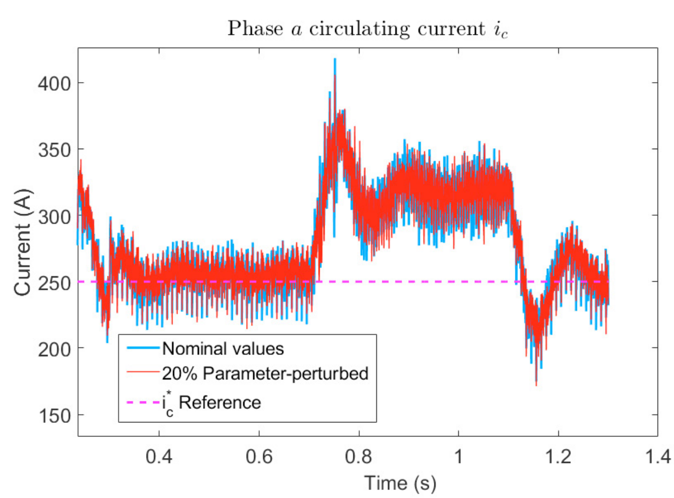

Fig. 8. Numerical results for i_c current: comparison between nominal case against parameter-perturbed case